Remote Sensing of Environment 157 (2015) 58–71

Contents lists available at ScienceDirect

Remote Sensing of Environment

journal homepage: www.elsevier.com/locate/rse

A satellite-based multi-temporal assessment of the extent of nuisance *Cladophora* and related submerged aquatic vegetation for the Laurentian Great Lakes

Colin Brooks *, Amanda Grimm, Robert Shuchman, Michael Sayers, Nathaniel Jessee

Michigan Tech Research Institute (MTRI), Michigan Technological University, 3600 Green Ct., Ste. 100, Ann Arbor, MI 48105, USA

ARTICLE INFO

Article history:
Received 19 December 2013
Received in revised form 17 April 2014
Accepted 28 April 2014
Available online 5 July 2014

Keywords:
Cladophora
Great lakes
Landsat
Submerged aquatic vegetation
Algae

ABSTRACT

In the Laurentian Great Lakes, the prolific growth of submerged aquatic vegetation (SAV, dominated by the filamentous green alga *Cladophora*) is negatively impacting human and wildlife health, fisheries, and aesthetic conditions. The distribution of *Cladophora* and similar SAV in the Great Lakes and how that has changed over recent decades has been unknown, and the magnitude of the current problem relative to historic growth is difficult to assess given the lack of field data and monitoring. Here, we present the first comprehensive map of SAV in the nearshore zone of the lower four Great Lakes, where 'nearshore' indicates the zone where the bottom reflectance is sufficient to characterize bottom substrate type, using primarily the visible bands of the Landsat TM sensor. Multiple spectral bands were combined to minimize the water-depth-dependent variance in lake bottom reflectance, and pixels were classified as dense vegetation, sparse vegetation or uncolonized substrate. Changes in vegetation cover and water clarity between the mid-1970s and present were also evaluated for several focus areas across the lakes utilizing historical Landsat TM and MSS imagery. The Landsat-based bottom classification achieved an overall accuracy of 83% based on comparison to ground truth data. Lake-wide SAV cover ranged from 15% (Lake Huron) to 40% (Lake Ontario) of the mappable lake bottom based on detection depth. The total mapped area of vegetation corresponds to a conservative biomass estimate of 129 kilotonnes dry weight. The observed changes in the distribution of SAV over time indicate that increasing water clarity in the Lakes is expanding *Cladophora* habitat.

1. Introduction

The native, filamentous green alga *Cladophora* (primarily *C. glomerata*) is one of the most common nuisance species in the Great Lakes (Auer et al., 2010). Under favorable conditions, this benthic alga can achieve dense growth on bedrock, cobble and other suitable hard substrates in the nearshore zone where sufficient light can reach the lake bottom (Hecky et al., 2004). The prolific growth of *Cladophora* and other submerged aquatic vegetation (SAV) fouls beaches and water intakes, impacting human and wildlife health, aesthetics, regional economics and other ecosystem services provided by the Lakes (see review by Higgins et al., 2008). *Cladophora* has also recently been reported as a food source for the Asian carp *Hypophthalmichthys molitrix*, and thus, the recent resurgence of nuisance *Cladophora* growth is likely to facilitate the establishment of this invasive species in the Great Lakes, a major ecological and economic concern (Rasmussen, Regier, Sparks, & Taylor, 2011).

Cladophora is a 'spring species,' growing well in cooler waters and senescing under the warm, bright conditions of the Great Lakes summer (Auer, Canale, Grundler, & Matsuoka, 1982; Graham, Auer, Canale, & Hoffmann, 1982). Episodic wind events occurring during the period of senescence lead to sloughing (detachment). Mats of floating, sloughed *Cladophora* are then transported toward shore, where they foul cooling water intakes and wash up on beaches, degrading aesthetics and reducing recreational value. Mats of sloughed *Cladophora* have been found to contain elevated levels of fecal indicator organisms (Nevers, Byappanahalli, Edge, & Whitman, 2014) and provide an anaerobic environment favorable to the growth of the bacteria responsible for avian botulism (Byappanahalli & Whitman, 2009). It is inarguable that the prolific growth of *Cladophora* and other SAV is a serious problem in the Great Lakes; that the problem manifests itself precisely where stakeholders encounter the Great Lakes makes SAV a critical endpoint in public assessment of management efforts aimed at improving and protecting the quality of the ecosystem.

It is important to note that *Cladophora* is not an invasive species. The alga was described as a component of the Great Lakes ecosystem in the early decades of the 19th century (Taft & Kishler, 1973), with reports of nuisance conditions occurring as early as the 1930s (Neil & Owen, 1964). Massive *Cladophora* blooms associated with anthropogenic nutrient enrichment, specifically increases in phosphorus concentrations, were common from the 1950s through the early 1980s across the

* Corresponding author. Tel.: +1 734 913 6858.
E-mail address: cnbrooks@mtu.edu (C. Brooks).

http://dx.doi.org/10.1016/j.rse.2014.04.032
0034-4257/

lower four Great Lakes (Neil & Owen, 1964; Herbst, 1969; Painter & Kamaitis, 1987; Auer et al., 1982). Although management of *Cladophora* was not an explicit focus for the Great Lakes phosphorus control strategies of the 1970s (detergent bans and limits on phosphorus discharges from municipal wastewater treatment plants), it was expected that successes achieved in offshore waters would be manifested in the nearshore as well. The program was considered a success, with reductions in phosphorus in Lake Ontario (see Higgins et al., 2008), for example, engendering a concomitant response in observed levels of *Cladophora* biomass (Painter & Kamaitis, 1987).

The contemporary resurgence in nuisance growth of SAV, predominantly *Cladophora* with localized areas of macrophytes, *Chara*, and diatoms (Malkin, Guildford, & Hecky, 2008; Stewart & Lowe, 2008), made manifest through beachfront accumulation of sloughed biomass, has been linked to the impacts of dreissenid mussels on water transparency (Auer et al., 2010; Tomlinson, Auer, & Bootsma, 2010). Zebra and quagga mussels, members of the genus *Dreissena*, invaded and colonized the Great Lakes in the early and mid-1990s and are now estimated to number in the hundreds of trillions in Lake Michigan alone (Fahnenstiel, Nalepa, & Pothoven, 2010). The filtering activities of mussels have lowered phytoplankton biomass in the Lakes, increasing water clarity (depth of the euphotic zone) and expanding suitable habitat for *Cladophora* and other SAV taxa into deeper water (Malkin et al., 2008). Additionally, it was anticipated that soluble reactive phosphorus concentrations near mussel beds would be elevated as a result of mussel excretion, i.e., "nearshore shunt" (Hecky et al., 2004). Where dreissenids are particularly dense, the accumulation of mussel shells is extending the area of colonizable hard substrate in the nearshore zone (Stewart, Miner, & Lowe, 1998). It is likely that these multiple impacts are enhancing the importance of benthic primary production relative to pelagicproduction in the Great Lakes, suggesting a major shift in carbon and nutrient flows (Malkin, Bocaniov, Smith, Guildford, & Hecky, 2010; North et al., 2012).

Phosphorus reductions, beyond those already in place in the Great Lakes region, are currently the only feasible means of addressing SAV problems. Changes in SAV aerial extent and biomass are the primary measures of the efficacy of such management efforts. To date, there has been no basin-wide assessment of the extent or biomass of SAV, primarily because *in situ* surveys of a basin the size of the Great Lakes are infeasible and cost-prohibitive. Because of this lack of field data and monitoring, the magnitude of the current problem relative to historic growth is difficult to assess.

Mapping various types of SAV has long been of interest based on attributes of the vegetation itself (e.g., nuisance and desirable/commercially valuable species) as well as the capacity of SAV to serve as a measurable indicator of ecological conditions. Previous work has demonstrated the feasibility of mapping SAV cover, including *Cladophora*, using satellite imagery (e.g., Lekan & Coney, 1982; Hochberg & Atkinson, 2003; Vahtmäe, Kutser, Martin, & Kotta, 2006; Kutser, Vahtmäe, & Martin, 2006; Shuchman, Sayers, et al., 2013), sometimes estimating biomass (Andréfouët, Zubia, & Payri, 2004) and determining change over time (Dekker, Brando, & Anstee, 2005). Benthic vegetation mapping using multispectral imagery is typically limited by water clarity and the limited spectral resolution of multispectral sensors, which can lead to confusion of pixels representing SAV, deep water and dark substrate types (e.g. muck) (Wolter, Johnston, & Niemi, 2005). Because of this potential for confusion, a reasonable level of knowledge of the study area and potential confounding influences is required. Previous imagery-based SAV mapping efforts in the Great Lakes Basin have been limited in extent to the southern shoreline of Lake Ontario: first using ERIM M-7 airborne multispectral imagery in the mid-1970s as part of the International Field Year on the Great Lakes program (Wezernak & Lyzenga, 1976) and again recently using imagery from AVIRIS and the airborne RIT MISI sensor (Vodacek & Raqueno, 2002). A comprehensive mapping effort on the scale of the nearshore regions of the Laurentian Great Lakes has not been undertaken. Methods have been developed to detect and characterize *Cladophora* beds in the Great Lakes using a high-frequency echosounder (Depew, Houben, Guildford, & Hecky, 2011). This approach provides valuable information on stand height that cannot be derived from multispectral imagery, but requires a vessel-mounted sensor that is not easily scaled up to regional mapping and thus this type of survey has been limited to selected shoreline areas (Depew et al., 2011).

The purposes of the mapping study described here were to 1) document the current distribution of SAV in the Lakes, and 2) provide a baseline from which to validate the effectiveness of future water quality management decisions. Historic satellite images from the Landsat archive dating back to the mid-1970s were used to construct a time series of SAV maps for focal areas distributed across Lakes Michigan, Huron, Ontario and Erie. Studies that utilize the satellite imagery archives now available to understand long-term changes in benthic cover are fairly uncommon; similar Landsat-based time series have been constructed to map the distribution of seagrass cover over time for certain marine and estuarine environments using different classification methods (Lyons, Phinn, & Roelfsema, 2012, Lyons, Roelfsema, & Phinn, 2013; Dekker et al., 2005; Knudby, Newman, Shaghude, & Muhando, 2010) but have reported average overall mapping accuracies generally lower than those reported here. Also, those study areas cannot be assumed to be optically similar to the inland, freshwater Great Lakes.

The time series presented here were queried to better understand how SAV distribution and the bottom detection depth limit (the deepest water in which the lake bottom reflectance is strong enough to characterize the bottom type, a measure of water clarity) have changed in recent decades and to evaluate the following hypotheses related to management and perturbation of the Great Lakes ecosystem:

- Phosphorus control efforts, resulting in lake-wide reductions in total phosphorous concentration that became apparent in the 1980s (DePinto et al., 2006), were accompanied by a proportional reduction in SAV/*Cladophora* area, but mussel-driven increases in water clarity have returned this area to pre-reduction levels or greater.
- The beginning of the resurgence in SAV cover in each lake temporally corresponds with mussel-driven increases in water clarity that coincide with the introduction of invasive dreissenid mussels into the lakes in the early 1990s (Nalepa & Schloesser, 2013).
- In recent decades, SAV cover has increased both in shallow (<10 m) areas and in deeper water where abundant growth has not previously occurred, resulting in a historic high in the total mapped area of SAV.

To evaluate the above hypotheses, we use a classification method adapted from Lyzenga (1981) to generate a basin-wide map of present-day SAV distribution ("baseline map") using recent (2008–2011) Landsat TM satellite imagery. The accuracy of this map is evaluated based on ground truth data, and the total area mapped as SAV is used to derive a first estimate of the total biomass of SAV in the Great Lakes based on typical *Cladophora* biomass densities. We then extend the classification methodology to estimate the trends in the distribution of SAV cover at selected sites across the Great Lakes basin.

2. Methods

2.1. Study site selection and descriptions

Apart from the baseline map, additional Landsat scenes dated 1973–2005 were acquired to generate time series maps of SAV cover distribution for five focal areas (Fig. 1). Study sites with a history of beach fouling by sloughed *Cladophora* and existing in situ data on the characteristics of SAV were selected to represent a range of conditions across the basin. Three focal areas (Bruce Peninsula in Lake Huron; Port Maitland, Ontario in Lake Erie; Ajax, Ontario in Lake Ontario) included or were located adjacent to sites where Depew, Stevens, Smith, & Hecky, 2009 recently conducted acoustic surveys of SAV in 2011. As part of a feasibility study that preceded the work reported here, we

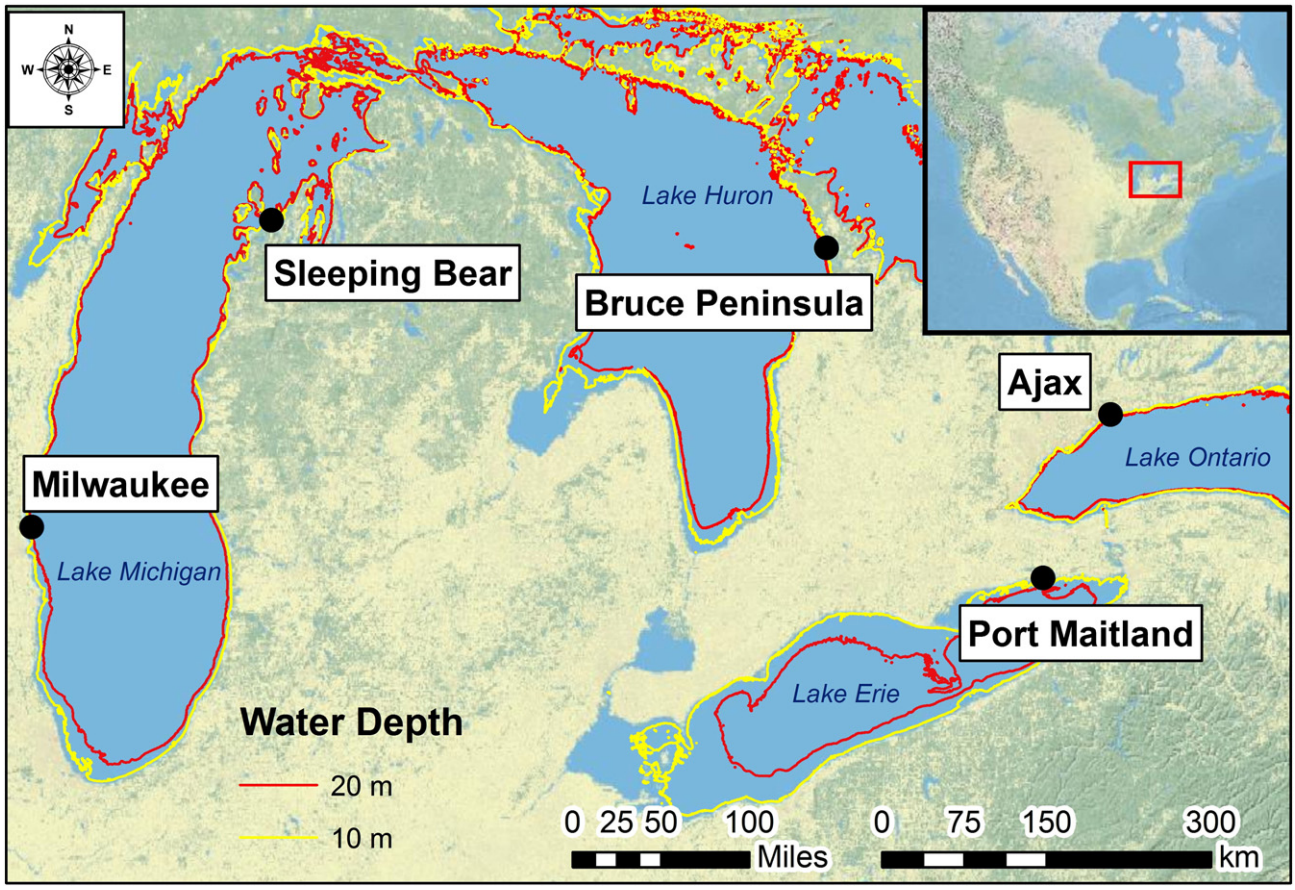

Fig. 1. Locations of the five focus areas for which time series were constructed.

collected SAV samples at a fourth area, Sleeping Bear Dunes National Lakeshore in Lake Michigan (Shuchman, Sayers, et al., 2013). SAV abundance at the last focal area, Milwaukee, Wisconsin (Lake Michigan), has been reported by Bootsma, Young, and Berges (2004).

The focal areas selected for the time series analysis differed considerably in terms of coastal land use. The shorelines near the Sleeping Bear Dunes and Bruce Peninsula focus areas are only lightly developed; a long section of coastline is protected at the former location as a National Lakeshore, and the latter was located on the west side of the Bruce Peninsula, where the land cover is dominated by forest with contributions from low-intensity agriculture and development (Depew et al., 2011). The coastal areas closest to the Port Maitland focal area are heavily dominated by agricultural land uses (Higgins, Howell, Hecky, Guilford, & Smith, 2005). The Ajax and Milwaukee sites are highly urbanized with an accompanying higher density of coastal development, shoreline hardening and sewage outflows.

The littoral substratum at the Bruce Peninsula and Port Maitland focal areas is dominated by bedrock and glacial till (Thomas, Kemp, & Lewis, 1973; Rukavina, 1970). The Ajax substratum is also primarily bedrock, with significant components of softer (sand, clay) substrates (Depew et al., 2011). The broad, shallow shoals offshore from Sleeping Bear Dunes are a mixture of unconsolidated glacial outwash and sand (Chambers & Upchurch, 1979). Finally, the littoral substratum near Milwaukee is characterized by bedrock with a thin cover of sediment (Cherkauer & Zvibleman, 1981).

2.2. Satellite imagery selection and processing

To generate a recent time period set of baseline lake-wide maps, fifty-six Landsat scenes (all Landsat 5) were selected, dating between 2006 and 2011. Most nearshore areas (over 90%) were mapped using images from 2008–2011; imagery from 2006 and 2007 was used sparingly as needed to fill in small areas where more recent imagery was not suitable, typically because of chronic water column disturbance. Scenes were collected between spring and summer (April to September); this time frame is supported by a seasonal analysis performed as part of this study. As reported in the project final report (Shuchman, Brooks, et al., 2013), seasonal comparisons were made at Sleeping Bear Dunes National Lakeshore (Michigan) and the area north of Milwaukee, WI. Cloud-free images from several dates within the same year were classified for each site (see Shuchman, Sayers, et al., 2013). The classifications generated from the different dates were then compared to assess how SAV varies seasonally and thereby define an appropriate seasonal window for selecting images that represent typical SAV cover during the growing season. The seasonal analysis showed that SAV extent, as detected by Landsat Thematic Mapper sensors, is relatively constant over the growing season. At the Sleeping Bear site, the proportion of the visible lake bottom classified varied from 31% in April, 28% in May, 33% in June, 35% in July, 35% in August, and 31% in early October using 2010 imagery (Shuchman, Brooks, et al., 2013). At the Milwaukee site, seasonal variation using 2009 imagery ranged from 30 to 34% for all dates using four May through September dates. Based on this evidence, the project team was able to use a single image collected for a lake in any given year as representative of the general conditions for that year.

For the time series maps of the five selected focal areas, a series of eight images was selected for each area representing the nearshore condition of the focal area at approximately five-year intervals from 1975–2010. Because Landsat 5 was not operational until the early 1980s, Landsat 1 through 3 (Multispectral Scanner System, MSS) imagery was used to characterize the focal areas circa 1975 and 1980. For both the baseline map and the time series, a set of cloud-free images

was chosen to represent the conditions with the largest area of visible nearshore areas captured within the specified date range.

SAV areas were mapped using an approach known as the SAV Bottom Mapping Algorithm (SAVMA, Shuchman, Sayers, et al., 2013), which was modified from the Lyzenga water column correction technique (Lyzenga, 1981; Lyzenga, Shuchman, & Arnone, 1979, Lyzenga, Malinas, & Tanis, 2006). The algorithm relies on the assumption that bottom reflected radiance is a function of bottom reflectance and an exponential function of water depth.

Bottom radiance linearized with respect to depth can be achieved for shallow water areas by the following equation:

$$Xi = Ln(Li - Lsi) \quad (1)$$

Where

Li = satellite pixel radiance for band i
Lsi = average radiance over deep water for band i, where there is no contribution from bottom reflectance
Xi = bottom radiance linearized with respect to depth for band i

This technique essentially normalizes the effect of varying water column depth on bottom reflected radiance (which now varies linearly with depth). Furthermore, if the linearized bottom radiance at two different bands, Xi and Xj, are plotted against each other, the points will fall along the same line given the same bottom reflectance. When there are *n* bottom types in a scene there will be *n* parallel lines for each bottom type that are displaced from each other in the plot. The y-intercept value calculated for each line from the band pair plots described above is assigned to each pixel in the image as seen in the equation:

$$yi = Ln(Li\text{-}Lsi) - [(Ki/Kj) * Ln(Lj\text{-}Lsj)] \quad (2)$$

where

Ln(Li–Lsi) = linearized bottom radiance
Ki/Kj = water attenuation coefficient ratio between bands i and j

A single image representing the band pair plot y-intercepts (yi) can be calculated from two visible spectrum bands of a given sensor. In the case of Landsat Thematic Mappper imagery, three y-intercept images can be created from the following band combinations: (blue and green, blue and red, green and red). These three images can then be subjected to a variety of image processing techniques to help differentiate bottom types even further.

Note Eqs. (1) and (2) assume that the shallow water radiance, Li, is greater than the deep water radiance, Lsi, indicating the lake bottom is visible. When Lsi is greater than or equal to Li we assume a deep water radiance for that location (i.e. bottom is not visible).

The method described above is a variation of the depth invariant index described by Lyzenga (1981):

$$Y = [Kj * \ln(Li\text{-}Lsi) - Ki * \ln(Lj\text{-}Lsj)]/\mathrm{sqrt}\left(Ki\text{^}2 + Kj\text{^}2\right)$$

The Lyzenga depth invariant index is a measure of the orthogonal displacement of the parallel lines observed in the band pair plots discussed above. In theory this approach is optimal to differentiate the multiple bottom types from a satellite image providing the parallel lines are clearly separable at the y-intercepts. In practice, particularly in some areas of the Great Lakes, the orthogonal displacement of the two lines representing SAV and sand is less well defined. This is due to the sand bottoms in the Great Lakes having lower spectral albedo as a function of the sand source (i.e. glacial deposits) and the presence of thin layers of decaying organic material. Thus the Great Lakes scenario is different from what is experienced in the Lyzenga Bahamas test site (Lyzenga, 1981) where the sands are a product of the coral carbonate life cycle and there is little to no terrestrial input of organic material to impact the sand albedo. Therefore, when the Lyzenga depth invariant index was applied to certain test sites in the Great Lakes, image classifications were unsatisfactory because the orthogonal displacement of lines is not well defined at all depths. Thus, a y-intercept threshold was determined from in situ observations of sand and SAV bottom types. This threshold was applied to the y-intercept images produced from Eq. (2), effectively assigning pixels below this threshold as SAV and above as sand/and or other uncolonized substrate.

The spectral albedo of very dense SAV is quite low as light is absorbed by the vegetation for the process of photosynthesis. The spectral albedo can be so low that the radiance values observed from satellite bands used in the SAVMA that when the Eq. (1) is applied, imaginary values occur. This is due to the SAV being "darker" than the nearby optically deep water and the subtraction of the two produces a negative value which is then imaginary when the natural log is applied. When this situation occurs within the range of bottom detection depth (determined from uncolonized substrate areas) those pixels are classified as SAV.

The ratio of band attenuation coefficients, Ki/Kj, can be derived from a given satellite image by comparing the bottom reflectance over varying depth for a single bottom type by:

$$Ki / Kj = a + (a2 + 1)1/2$$

where

$$a = (\sigma ii - \sigma jj) / 2\sigma ij$$

and

σii = variance of Xi
σij = covariance of Xi and Xj

This approach is ideal, but requires the manual selection of pixels of a given bottom type at different depths to reconstruct the attenuation coefficients. Because the overall goal in the generation of the SAVMA was to produce a Great Lakes basin wide SAV distribution map, the additional scene specific water attenuation processing requirement is not ideal. Instead, for this study, the water attenuation coefficients for Landsat bands were assumed a priori using water column optical profiles for the Great Lakes collected in situ in 2008 using Satlantic's HyperPro II, a hyperspectral radiometer (Satlantic, Halifax, Nova Scotia). Separate ratios were calculated for the western basin of Lake Erie (i.e., west of the Lake Erie Islands) and the rest of the lake. The attenuation coefficients used for each lake are presented as Table 1.

To assess the error introduced by applying in situ measurements of attenuation for all imagery, a comparison was made between a set of in situ attenuation ratio coefficient measurements made in Lake Michigan and those derived from several Landsat scenes throughout the growing season over the Sleeping Bear Dunes National Lakeshore area in Lake Michigan. The results showed little variation between the in situ ratios and those derived from each scene, indicating for this test area that the water color producing constituents were not varying significantly in the growing season (data not shown). Therefore an average attenuation ratio was determined to be sufficient for this analysis.

Atmospheric conditions are very dynamic in the Great Lakes, particularly near shore in the warmer months where a water/land temperature

Table 1
Water attenuation coefficient ratios (Landsat 5 band 1/band 2) for each lake derived from field data collected in 2008 with a hyperspectral radiometer.

Lake	Attenuation ratio	Standard deviation
Michigan	0.36	0.25
Huron	0.61	0.19
Erie (West)	1.09	0.04
Erie (East)	0.76	0.07
Ontario	1.07	0.06

gradient occurs. Because of this, several different atmospheric conditions can be encountered within a given satellite image. This makes applying Eq. (1) with deep water radiance pixels (Lsi) in one atmospheric condition to pixels (Li) that have significantly different atmospheric conditions erroneous, as the potential for negative values exists in areas that are optically shallow. Moreover, the lack of cloud free Landsat data in the Great Lakes during the growing season (~4 images/year) doesn't allow for the selection of only the least atmospherically contaminated pixels from several images to be joined as many areas along the basin shorelines will be incomplete. To circumvent this deficiency, cloud-free Landsat images were broken into regions with similar atmospheric conditions. These regions must contain both deep water radiance pixels and optically shallow pixels. We calculate Lsi from a sample of pixels adjacent to the portion of the shoreline being mapped with 1) similar atmospheric conditions and 2) a water depth of at least 30 m (less in Lake Erie and Saginaw Bay where the whole basin is very shallow and the bottom depth detection limit is small). The SAVMA is then applied to each region separately, with the classified output being mosaicked together.

Finally, a 9×9 Gaussian convolution function was used to reduce speckling in each y-intercept raster. Using gridded Great Lakes bathymetry layers (Schwab & Sellers, 1996), the maximum water depth reached by the finished y-intercept rasters (here termed bottom detection depth limit, as opposed to optical depth) could be quantified for all mapped areas.

2.3. Image classification

The methods developed in Shuchman, Sayers, et al., 2013 for the Sleeping Dunes National Lakeshore in Lake Michigan were extended to the larger nearshore areas of Lakes Michigan, Huron, Erie, and Ontario. The band pair y-intercept image values were classified as 'dense SAV' ($\geq$75% SAV cover), 'less dense SAV' ($\geq$25% SAV cover) and 'bare substrate' (<25% SAV cover) bottom types. Pixels that were located in nearshore areas (detection depth) with low radiance values but were spectrally similar to deep water pixels based on the band pair y-intercept images were classified as 'dense SAV'. The threshold between the 'less dense SAV' and 'bare substrate' bottom types was selected based on ground truth bottom type data and interpretation of the natural color Landsat imagery. If significant areas that the interpreter did not confidently believe to represent SAV were assigned to an SAV class, i.e., that may be explained by the presence of an observed bloom of phytoplankton obscuring the water column, a better image from that path/row was obtained. Finally, all classified images were mosaicked together to create a continuous bottom type map for the nearshore zone of each lake.

The above procedure was used to generate the baseline map of the current distribution of SAV cover across the entire basin and time series maps for the five identified focal areas dating back to the mid-1980s; to further extend our time series to the mid-1970s, Landsat MSS imagery collected by Landsat satellites 1-3 was used. MSS imagery could not be converted to the same band pair y-intercept rasters as the Landsat 5 imagery because the MSS sensor lacks a 'blue' spectral band (~0.4–0.5 μm). Thus, for MSS imagery, band 4 (green) was converted to bottom reflectance linearized with respect to depth using Eq. (1) and that single depth-linearized band was classified into bottom types in the same way that the band pair y-intercept rasters were classified for TM imagery. This alternative method results in a classification with a similar bottom detection depth limit but a coarser ability to differentiate between bottom types compared to the y-intercept images while enabling a longer historical analysis. A comparison of the SAV classification results from TM and MSS imagery for the same shoreline area and time period, resampling the TM data to MSS resolution, indicated that the results are very similar (pixel classifications were 96% identical).

2.4. Estimation of lakewide biomass

Estimates of lakewide biomass are developed as the product of the areal coverage of SAV and the biomass density characteristic of those areas. Satellite-based mapping of areal coverage is limited to optically shallow areas where bottom-reflected radiance is detectable by a sensor and it cannot be assumed *a priori* that SAV colonization does not extend beyond the limits of sensor detection. This issue was examined by applying the Great Lakes *Cladophora* Model (GLCM; Tomlinson et al., 2010) to calculate peak *Cladophora* biomass along a shore-perpendicular transect extending lakeward to the limit of light penetration (1% level) for a range of bottom detection depth limit values (1–20 m) characteristic of Great Lakes waters. Model inputs (incident light, temperature and soluble reactive phosphorus) were those used for model confirmation (Lake Michigan at Milwaukee, WI; Tomlinson et al., 2010). The vertical light extinction coefficient ($K_{PAR;}$ photosynthetically available radiation) was estimated using the relationship between Secchi disk transparency (SD) and K_{PAR} developed by Bukata, Jerome, Kondratyev and Pozdnyakov (1995), and SD was calculated as 50% of the bottom detection depth limit, using a relationship shown between green-band bathymetric LiDAR and SD (Guenther, Cunningham, LaRocque, & Reid, 2000). Model-predicted biomass was then partitioned between that residing at water depths less than the bottom detection depth limit (sensor visible) and that beyond the range of the sensor. These results were then used to calculate the fraction (f) of *Cladophora* detected, and that fraction was examined as a function of bottom detection depth limit. The value of f ranged from 0.6 at a bottom detection depth limit of 1 m (i.e., if the detection limit was 1 m. 40% was not visible to the satellite), to 0.8 at 10 m (if the detection limit was 10 m, then only 20% of *Cladophora* was not visible) to >0.9 at 20 m (values seen in Lake Michigan), averaging 0.8 ± 0.3 for the range of detection limits we experienced. These calculations assume that substrate is totally and equally colonized. However, we note that the value of f will increase where coverage by *Cladophora* decreases in deeper waters due to reductions in habitat colonization, a common occurrence due to deposition of sediment at such locations. Finally, we assume a linear increase in depth with distance offshore; however, the fraction of *Cladophora* sensed will increase for areas where extensive shallow regions (e.g. shoals) are present.

Biomass determined for the detection-visible region may be multiplied by a scaling factor ($1/f$) to provide an estimate of total biomass that includes the biomass present beyond the bottom detection depth limit; a value of 1.1, corresponding to a detection depth of 20 m, is used here. Lakewide biomass was calculated by multiplying the area mapped as SAV by estimates of SAV biomass density (gDW/m^2), seeking to capture the range of spatial and temporal variation in that density as influenced by variability in forcing conditions and the frequency and magnitude of sloughing events. The range is defined by a lower (nominal) bound of 50 gDW/m^2 and an upper bound of 100 gDW/m^2. Measurements of *Cladophora* densities lower than 50 gDW/m^2 and higher than 100 gDW/m^2 have been reported; however, the selection of these values as bounds for lakewide conditions is consistent with both measurements made by our team and published and unpublished densities reported by others (Bootsma et al., 2004; Depew et al., 2011; Higgins et al., 2005; Higgins, Pennuto, Howell, Lewis, & Makarewicz, 2012; VanSumeren et al. unpublished data). These nominal and high biomass values were applied to all pixels classified as SAV to arrive at SAV biomass estimates.

2.5. Field data collection

Field verification was conducted during the 2010–2012 growing seasons. Water depth, Secchi depth and lake bottom characteristics, specifically the presence/absence and percent cover of submerged aquatic vegetation (SAV), were documented at points near 11 field locations distributed throughout the four lower Great Lakes (Fig. 2). SAV percent cover was estimated using a color underwater video camera. Data from four sites (Saugatuck, MI; Harbor Beach, MI; Lake Erie

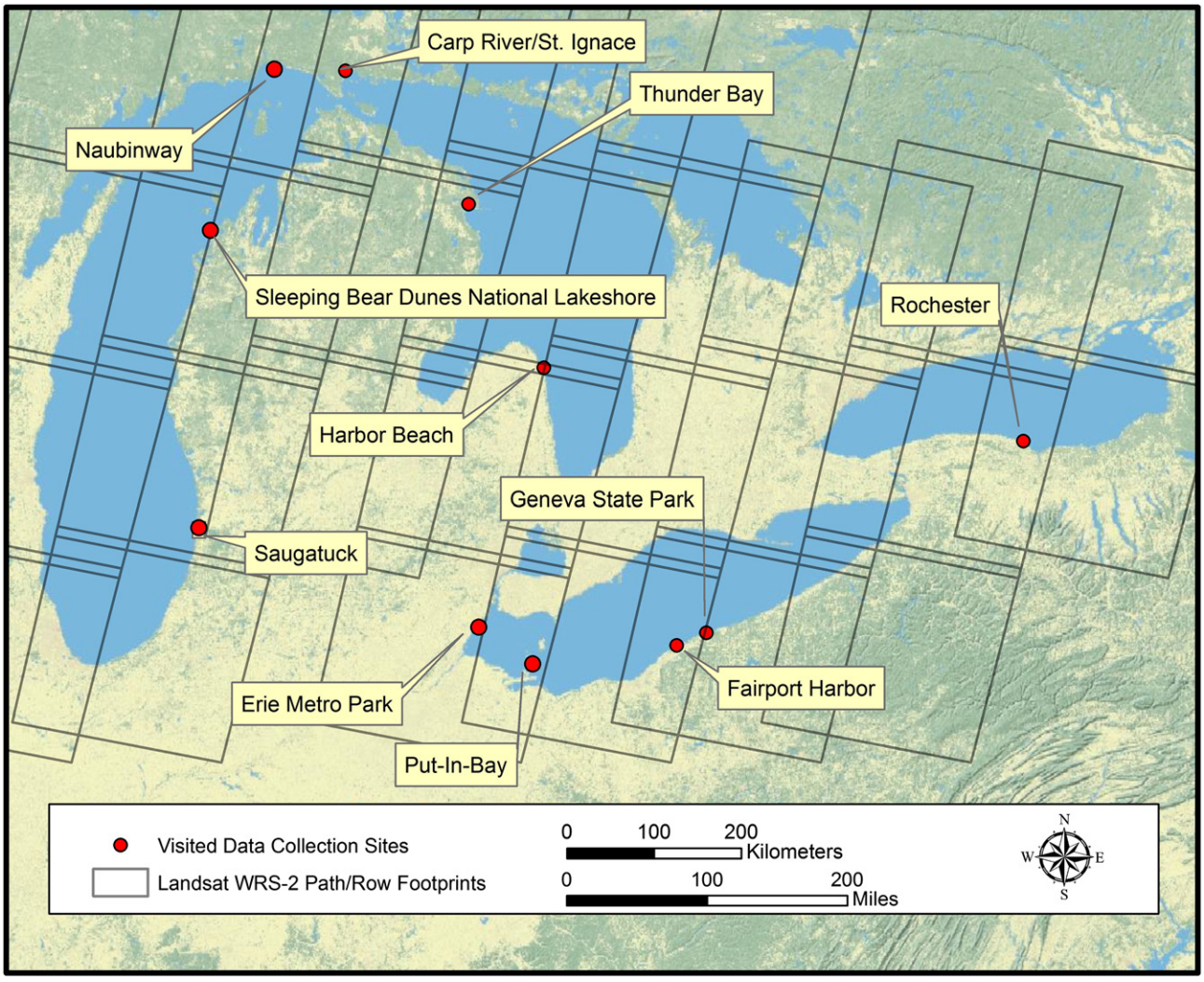

Fig. 2. Field locations visited during the 2010–2012 growing seasons.

Metropark, MI; Put-In-Bay, OH) were used as training data (total of 180 ground truth samples). The remaining 7 locations (320 ground truth samples) were utilized as validation data. We selected the number of samples needed to evaluate the classification accuracy based on the number of bottom types being mapped, the likely distribution of the types, and our a priori desired accuracy threshold of 80%, following Congalton and Green (2008). Our validation dataset also meets Congalton's "rule of thumb" for assessing the accuracy of remote sensing-based classifications of a minimum of 50 samples for each map class for maps of <1 million acres and fewer than 12 classes (Congalton, 1988). The likely distribution of bottom types was estimated from the initial feasibility study at Sleeping Bear Dunes described in Shuchman, Sayers, et al. (2013a).

Lake bottom types were documented using an underwater color camera and sub-meter capable GPS receiver; for a detailed description of field activities, see Shuchman, Sayers, et al., 2013; Shuchman, Brooks, et al., 2013.

3. Results

3.1. Baseline maps

Bottom type maps for the nearshore zone were generated for Lakes Michigan, Huron, Erie and Ontario using Landsat 5 imagery from primarily 2008-2011 (Fig. 3; maps in PDF format, plus an interactive mapping site, are available through http://www.mtri.org/cladophora.html). In the maps, SAV is represented in dark green (for dense areas) and light green (for less dense areas), and sand/uncolonized substrate is represented in beige. Other bottom types, if present, were not identifiable at the Landsat 30-m pixel resolution. The characteristics of each Lake's SAV map are summarized in Table 2, where 'total mapped area' indicates the total area of all Landsat pixels for which the lake bottom type could be classified in each lake. Much of the western basin of Lake Erie as well as small areas along the shoreline of Lake Huron could not be classified due to turbidity that consistently obscured the lake bottom.

3.2. Field validation of bottom map

MTRI visited 11 areas distributed across the four lower Great Lakes during the 2010-2012 growing seasons. Field validation points were categorized according to the percent SAV cover observed in the field: sites with 25% or greater SAV coverage were considered SAV sites and locations with SAV cover less than 25% were considered non-SAV. Tables 3 and 4 summarize all verification data collected for this project as a single tabulation of overall accuracy on a Lake-by-Lake basis and an error matrix representing the data from all field locations. The field verification activity resulted in 320 field observations being collected; of those, 266 were correct. The final basin-wide accuracy was 83.1%, similar to the accuracy results obtained in Shuchman, Sayers, et al., 2013;

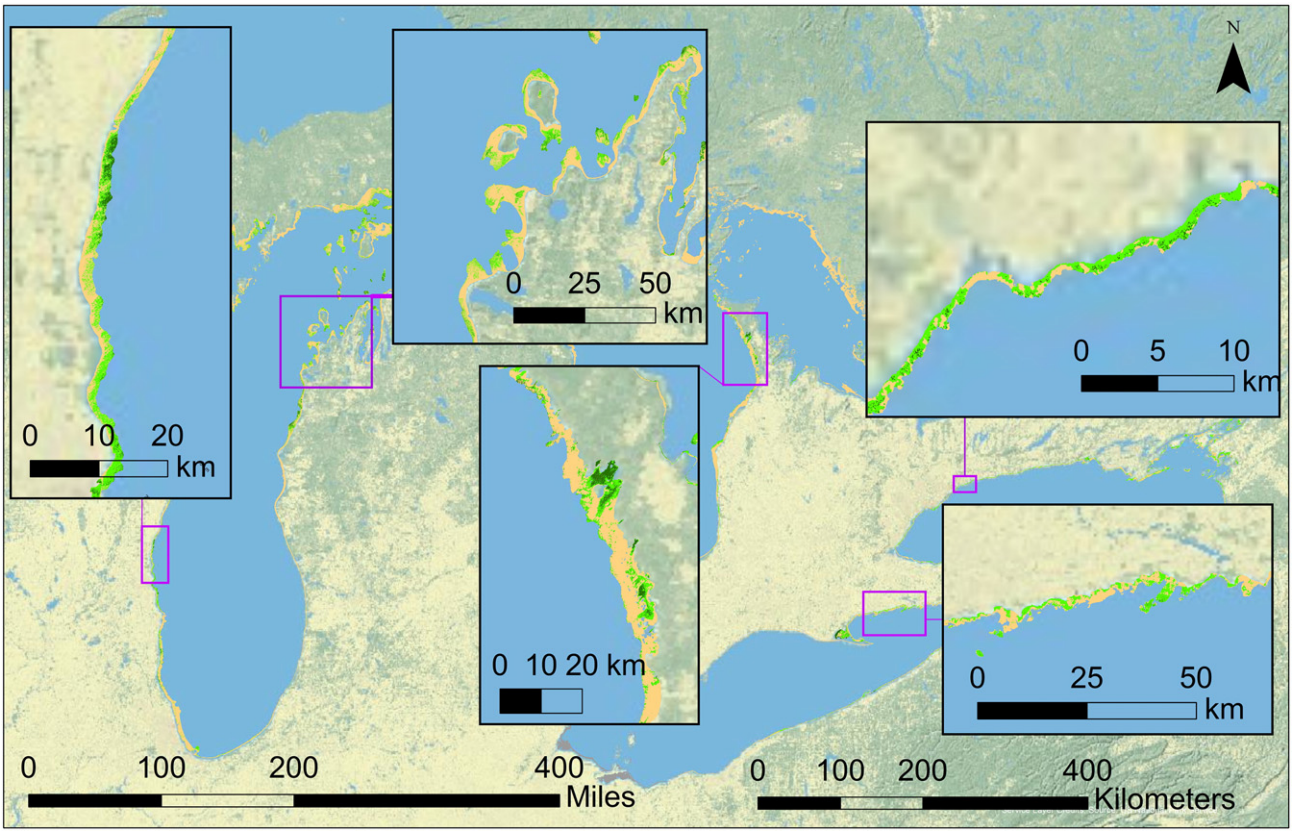

Fig. 3. Overview of the SAV maps created for the four lower Great Lakes with insets of (from left to right) Milwaukee, Bruce Peninsula, Ajax, and Port Maitland. Dark green corresponds to dense SAV, light green to less dense SAV, beige to uncolonized substrate, and gray to unclassifiable areas (e.g., in western Lake Erie).

Shuchman, Brooks, et al., 2013 for the initial mapping feasibility effort that was focused on Sleeping Bear Dunes National Lakeshore in Lake Michigan and the Ajax, ON shoreline in Lake Ontario.

3.3. Biomass estimates

Lake-wide dry weight estimates of SAV biomass were made using 50 gDW/m^2 as the nominal biomass estimate and 100 gDW/m^2 as an upper bound as described in the Methods. As noted, the Great Lakes *Cladophora* Model was used to examine that the percentage of cumulative annual net production of *Cladophora* observable by Landsat is approximately 90% or greater ($f > 0.9$) of total production for bottom detection depth limits are 20 m with similar values ($f = 0.8$) for other detection limits commonly seen in the Great Lakes. Based on these findings, total SAV (visible plus deep water growth) was estimated by multiplying the estimate of visible SAV by 1.1. Dry weights were converted to wet weights using a standard factor of ten (Piller, McArdle, & Patrick, 2008). Results are expressed as both visible and total biomass, where total biomass includes SAV/*Cladophora* beyond the bottom detection depth limit, and assumes that coverage of total mapped SAV area is equivalent there to that in the detection limit area. Total dry weight SAV biomass, summed for the four Lakes, ranged from 129 kilotonnes in the nominal case to 259 kilotonnes in the upper bound case (Table 5).

3.4. Time series analysis

Landsat scenes from at least eight dates distributed approximately every five years between the mid-1970s and 2010 were classified for each of the five focal areas in Fig. 3. Three metrics are utilized here in analyzing information derived from satellite imagery relative to SAV distribution and the light environment: area mapped as SAV, area mapped as uncolonized substrate, (their sum being the total mapped area) and bottom detection depth limit. Uncolonized substrate is interpreted as representing lake bottom that receives sufficient light to support *Cladophora* growth but features <25% SAV cover, either due to a lack of the solid substrate required for colonization by attached algae or to some other factor (e.g. nutrient limitation). This analysis also endeavors to place mapping results within the context of factors impacting or potentially impacting the area mapped as SAV. To that end, we divide the four-decade period examined here into three intervals: one representing conditions prior to manifestation of the results of P-loading reductions, a second following P-loading reductions but prior to widespread colonization by dreissenids, and a third representing conditions when dreissenid populations were well established. In Fig. 4

Table 2
Total mapped area, area of mapped SAV and percent cover of SAV for each lake.

Lake	Total mapped area (km2)	Area mapped as SAV (km2)	Percent SAV	Mean bottom detection depth limit (m)	Maximum bottom detection depth limit (m)
Michigan	4390	1220	28%	12	>20
Huron	4370	665	15%	9	20
Erie	530	160	30%	4	7
Ontario	790	315	40%	6	9

Table 3
Final overall classification accuracies on a Lake by Lake basis.

Lake	Overall accuracy
Michigan	83%
Huron	83%
Erie	83%
Ontario	84%

below, the SAV cover at each focal area is normalized relative to the "original" area in the first image of each time series (mid-1970s). The result clearly demonstrates the relative impacts of P-loading management and dreissenid activity of areal coverage by SAV. The timeline of response for each Lake is treated in detail in the following subsections. In Figs. 5-9, the total mapped area is separated into the 'standardized lake bottom area', meaning those pixels that could be classified in every image of the time series, and the remaining 'non-standardized area', pixels that were only classified in some images. This was done to enable evaluation of the same geographic area over time and the assessment of the relative importance of change in SAV cover at all depths vs. change in the depth to which SAV could be mapped, which based on the GLCGM, is strongly correlated with the depth to which SAV growth occurs.

3.4.1. Sleeping bear dunes national lakeshore—Lake Michigan

For the standardized lake bottom area (dark green + dark orange bars in Fig. 5), SAV cover at Sleeping Bear declined from approximately 29% in 1981 to just above 15% by 1990. After 1990, however, SAV patches expanded once again, exceeding their 1970s coverage to reach approximately 35% of the standardized area. When the nonstandardized (light green and orange) areas are taken into account, it is apparent that much of the increase in SAV cover for the total mapped area can be attributed to an increase in water clarity. While the percent SAV cover of the total mapped area has fluctuated between approximately 18 and 44%, the absolute area mapped as SAV has increased nearly four-fold; over the same time period, the total mapped area at this site increased more than three-fold due to the increase in water clarity.

3.4.2. Milwaukee, WI—Lake Michigan

Up until 1994, SAV coverage along the Milwaukee shoreline was approximately 10-15% for both the standardized and total areas with somewhat lower values in 1987 (Fig. 6). Like at Sleeping Bear, c.1994 represented an inflection point for SAV coverage along the Milwaukee lakeshore, which then increased steadily to >25% coverage. Mean bottom detection depth limit has also steadily increased near Milwaukee. From Fig. 6, it is clear that the increase in total area mapped as SAV was more strongly related to an increase in the percent cover of SAV (from approx. 9% in 1974 to 33% in 2009) than to the relatively modest increase in mappable area. In comparison with the Sleeping Bear Dunes site, nearshore bathymetry along the Milwaukee coastline is more strongly sloped, resulting in a narrower band of optically shallow water and a more limited increase in mappable area with increasing bottom detection depth.

Table 5
Dry and wet biomass estimates (visible and visible + deep water) for each lake. All estimates are in metric kilotonnes.

		Michigan	Huron	Erie	Ontario	Total
Nominal	**DW visible SAV**	61	33	8	16	118
	WW visible SAV	610	332	79	158	1179
	DW total SAV	67	36	9	17	129
	WW total SAV	671	365	87	174	1297
Upper bound	**DW visible SAV**	122	66	16	32	236
	WW visible SAV	1,220	664	158	317	2359
	DW total SAV	134	73	17	35	259
	WW total SAV	1,342	730	174	349	2595

3.4.3. Port Maitland, ON—Lake Erie

The pattern of change in SAV cover at Port Maitland (Fig. 7) was similar to that for the Lake Michigan sites, with a slight decrease in cover for the standardized area from the beginning of the time series to the end of the 1980s followed by a distinct increase. The increase in cover at Port Maitland began before 1990, which is slightly earlier than for the Lake Michigan sites. The northern shoreline of Lake Erie between Long Point and the Niagara River shows the greatest bottom detection depth limit; the wider optically shallow zone in this area, particularly the shoal west of Port Maitland, favors the growth of larger patches of SAV. Located at the eastern end of Lake Erie, the bottom detection depth limit at Port Maitland is greater than in Erie's western and central basins, showing a bottom detection depth limit increase on par with that observed near Milwaukee. The mean bottom detection depth limit for Lake Erie has nearly doubled, from ~5 m in the 1970s to more than 9 m in 2010. Looking at the change in total areas mapped as SAV and uncolonized substrate (Fig. 7), the increase in SAV area at Port Maitland appears to be the combined effect of simultaneous gradual increases in mappable area and percent cover of SAV.

3.4.4. Bruce Peninsula, ON—Lake Huron

The Bruce Peninsula was the only focal area to exhibit a decline in the percent cover of SAV over time (Fig. 8). The SAV cover for the standardized area in particular was higher from the 1970s to 1990 than for more recent dates. Percent SAV cover also decreased for the total mapped area, as total mapped SAV remained stable at approx. 40 km^2 but the total mapped area increased by approx. 50 km^2 over the course of the time series. Like the other areas of interest, water clarity has steadily increased along the Bruce Peninsula, with the mean bottom detection depth limit approximately doubling between 1975 and 2011.

3.4.5. Ajax, ON—Lake Ontario

The general pattern of change in SAV cover for the standardized area at Ajax in Lake Ontario is the same as for Lakes Michigan and Erie; a slight decrease in cover from the beginning of the time series to the 1990s followed by an expansion to greater than 1970s-level coverage (Fig. 9). The expansion began later at Ajax than at the other sites, with SAV extent still decreasing as late as 1997. The increase in water clarity, however, began in the early 1990s, consistent with the pattern seen at other sites (Figs. 7, 8).

Table 4
Error matrix produced from all the verification data used to assess the accuracy of the remote sensing SAV maps. Of the 320 field observations, 266 points (or 83%) were verified correct.

Map Classification	Field Observations					
	SAV	Non-SAV	Optically Deep	Total	User's Accuracy	Errors of Commission
SAV	154	12	3	169	91.1	8.9
Non-SAV	28	87	2	117	74.4	25.6
Optically Deep	6	3	25	34	73.5	26.5
Total	188	102	30	320		
Producer's Accuracy	81.9	85.3	83.3	Overall Accuracy		
Error of Omission	18.1	14.7	16.7	83%		

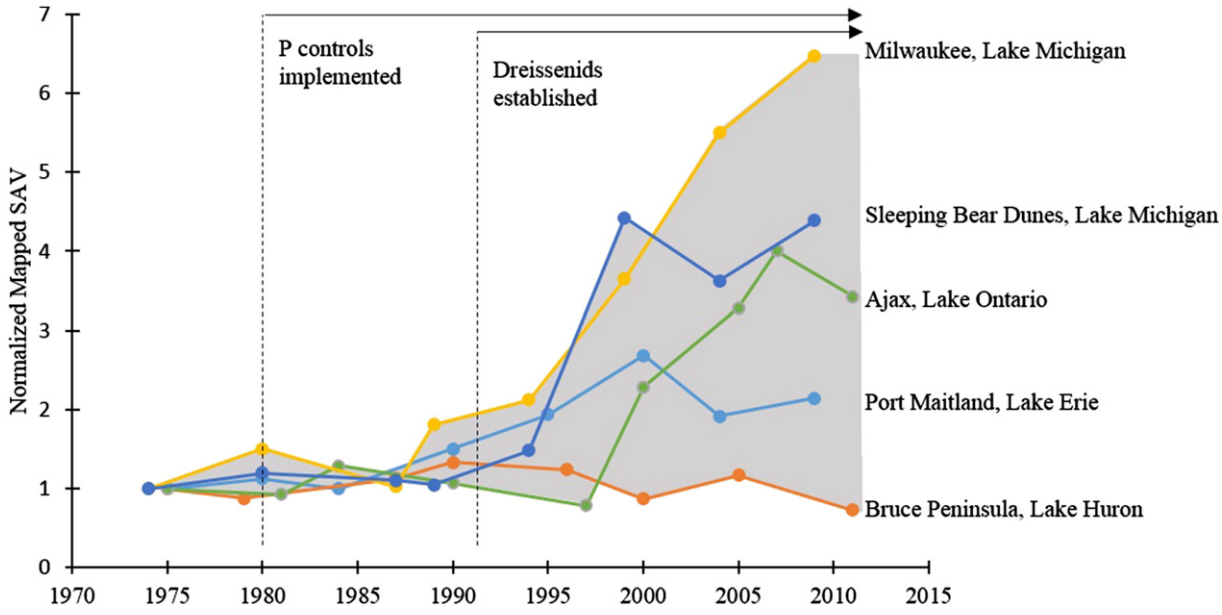

Fig. 4. Timeline of change in SAV area at the five focus areas, annotated with relevant events.

As Fig. 9 shows, the total mappable area at the Ajax site roughly doubled from 1975 to 2010, with the largest jump between 2000 and 2005. As a result of this increase, the total area mapped as SAV was distinctly larger after 2000 than on earlier dates.

4. Discussion

4.1. Current distribution of SAV

The overall accuracy of the baseline map of Lakes Michigan, Huron, Erie, and Ontario was approximately 83%, which is somewhat higher than has been reported for similar Landsat-based maps of seagrass cover (65%, Lyons et al., 2012; 76%, Dekker et al., 2005; up to 69%, Knudby et al., 2010). This indicates that our final map product is a fairly reliable resource for use in lake management and monitoring efforts, both for identifying the current extent and distribution of SAV and as a baseline distribution for evaluating future change. Water quality managers will be challenged to quantify and defend the efficacy of proposed phosphorus control strategies given the financial burden associated with enhanced wastewater treatment and further land use control, and monitoring changes in SAV extent and biomass is a direct measure of the efficacy of such strategies. The discussion below examines the response of the four Lakes to P management and colonization by dreissenids.

4.1.1. Lake Michigan

Four areas of especially concentrated SAV growth can be observed in the lakewide SAV map for Lake Michigan: Sleeping Bear Dunes National Lakeshore, Green Bay, the northern end of the lake west of the Mackinac Bridge, and Milwaukee. Of these, the first three are the shallowest areas of the lake, with depths of less than 10 m extending further into the lake interior than along most of the shoreline. Overall, these three areas are not adjacent to urban centers, though Green Bay is impacted by urban discharge via the Fox River. The presence of such dense *Cladophora* along Sleeping Bear Dunes National Lakeshore is incongruous, as much of the lakeshore is undeveloped and presumably less affected by

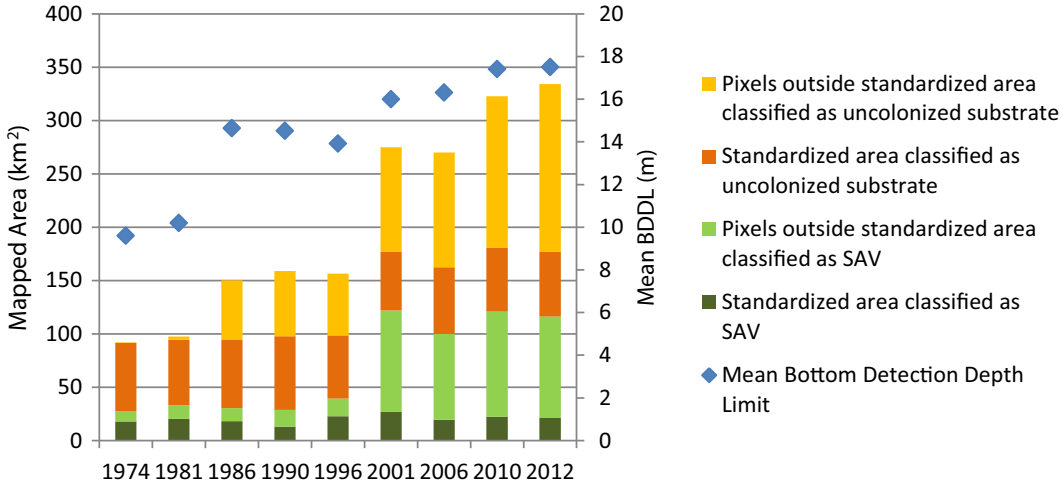

Fig. 5. The surface areas classified as SAV and as uncolonized substrate within and outside of the standardized lake bottom area, i.e., the pixels that were classifiable in all years of the time series, at Sleeping Bear Dunes National Lakeshore (Lake Michigan) from the 1970s to the present. Darker colors represent standardized-area pixels and lighter colors nonstandardized-area pixels. Blue diamonds represent the mean bottom detection depth limit within the focus area.

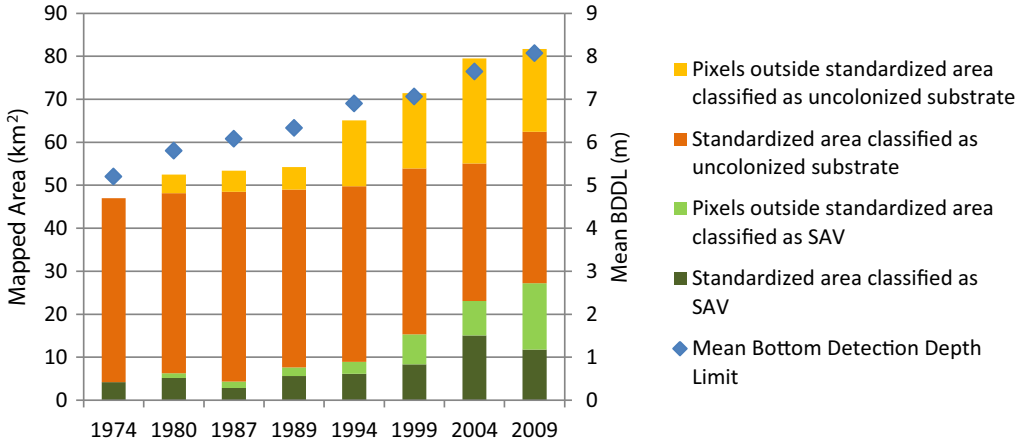

Fig. 6. The surface areas classified as SAV and as uncolonized substrate within and outside of the standardized lake bottom area, i.e., the pixels that were classifiable in all years of the time series, along the Milwaukee shoreline (Lake Michigan) from the 1970s to the present. Darker colors represent standardized-area pixels and lighter colors nonstandardized-area pixels. Blue diamonds represent the mean bottom detection depth limit within the focus area.

nutrient runoff. The presence of an SAV 'hotspot' at Sleeping Bear may be the result of the current flow in Lake Michigan carrying P to the Sleeping Bear area from more distant tributaries, the capture and recycling of allochthonous P by dreissenid mussels (Hecky et al., 2004), for which the shallow waters offshore from Sleeping Bear are ideal habitat, and/or an increasing availability of hard substrate provided directly by mussel beds forming on softer sediments. Previous field efforts, such as the ground truth data collected for Shuchman, Sayers, et al., 2013, have found that accumulations of dreissenid mussel shells have created new areas of hard substrate for *Cladophora* to colonize on the largely sandy bottom substrates near Sleeping Bear.

Studies of nearshore P cycling in the Great Lakes have reported conflicting results regarding whether dreissenids recycle sufficient P to sustain nuisance *Cladophora* growth in the absence of significant external loading (Makarewicz & Howell, 2012; Hecky et al., 2008). Based on the current SAV distributions mapped in this study, particularly in Lake Michigan, where the ambient P concentration has become quite low, the effect of dreissenid mussels on phosphorus cycling and light penetration in the nearshore zone appears to make it increasingly possible for SAV blooms to occur anywhere in the Great Lakes where the substrate is suitable. However, it is clear that urbanized coasts still serve as an important source of nutrients that can drive local SAV blooms. For example, SAV growth is much denser in the Milwaukee area than elsewhere along that region of the lakeshore.

Overall, the northern end of Lake Michigan exhibits the greatest bottom detection depth limit and the southeastern shoreline the shallowest bottom detection depth limit. Local bottom detection depth limit varies from 2 m to greater than 20 m.

4.1.2. Lake Huron

The percentage of the Lake Huron nearshore zone mapped as SAV was the lowest of all the lakes (15%), consistent with its limited and largely invariant phosphorus inputs. The baseline map for Lake Huron indicates smaller and more isolated SAV beds relative to Lake Michigan. The occurrence of individual beds at specific locations cannot be confidently ascribed to local phosphorus sources, phosphorus recycling by mussels and/or patchiness of hard substrate at this time. The densest areas of growth were found in the extreme north of the lake near Bois Blanc Island, MI; between Mackinac Island and Alpena, MI; along the western shoreline of the Bruce Peninsula; and in Saginaw Bay. Although not field verified here, SAV in northern Lake Huron is dominated by *Cladophora* but is also known to include *Chara* as a subdominant species, representing approximately 10% of the SAV cover (Sheath, Hambrook, & Nerone, 1988). The Bruce Peninsula in particular has been a hotspot for

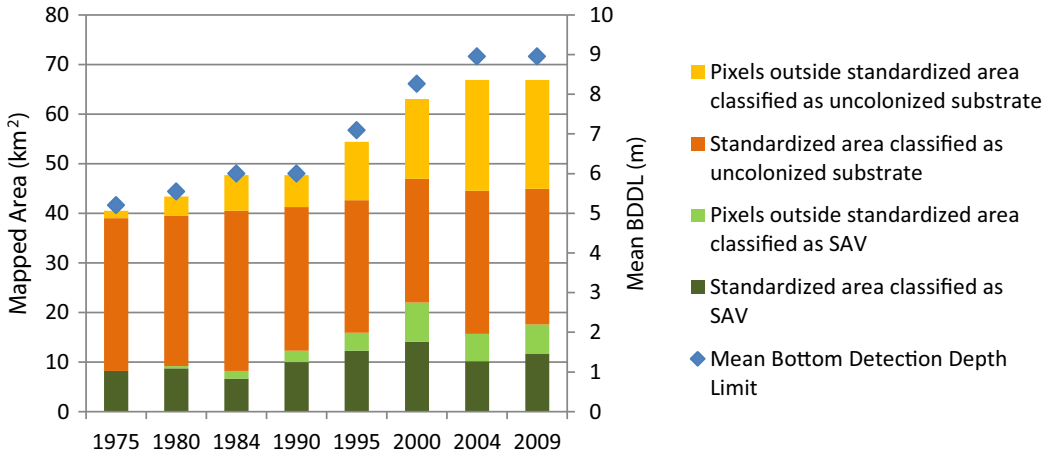

Fig. 7. The surface areas classified as SAV and as uncolonized substrate within and outside of the standardized lake bottom area, i.e., the pixels that were classifiable in all years of the time series, along the Port Maitland shoreline (Lake Erie) from the 1970s to the present. Darker colors represent standardized-area pixels and lighter colors nonstandardized-area pixels. Blue diamonds represent the mean bottom detection depth limit within the focus area.

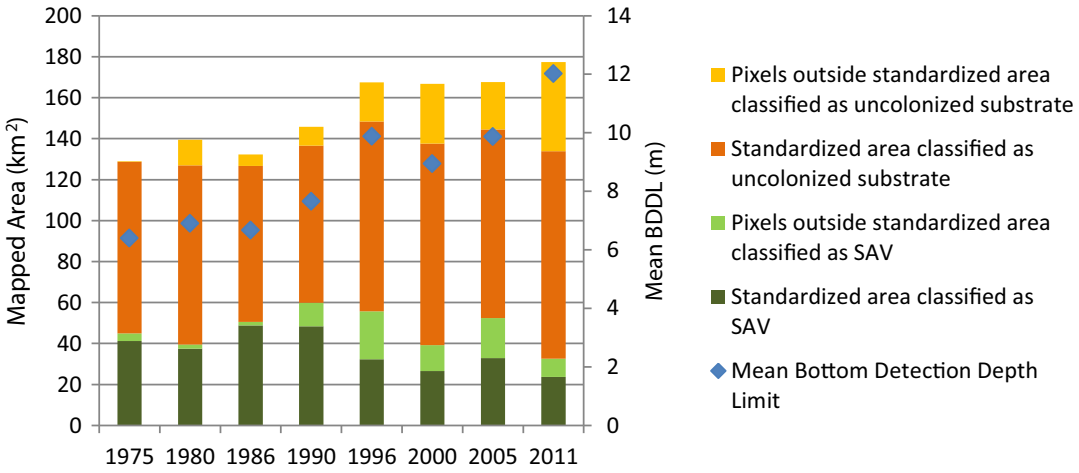

Fig. 8. The surface areas classified as SAV and as uncolonized substrate within and outside of the standardized lake bottom area, i.e., the pixels that were classifiable in all years of the time series, along the Bruce Peninsula shoreline (Lake Huron) from the 1970s to the present. Darker colors represent standardized-area pixels and lighter colors nonstandardized-area pixels. Blue diamonds represent the mean bottom detection depth limit within the focus area.

botulism-related bird die-offs, possibly linked to *Cladophora* blooms (U.S. EPA, 2008). The history of *Cladophora* in Lake Huron is somewhat different from the other lower Great Lakes; whereas *Cladophora* growth was prolific during the 1950s–1970s on submerged hard surfaces throughout Lakes Michigan, Erie, and Ontario, ambient nutrient concentrations in Lake Huron were not sufficient during that period to support extensive growth, and *Cladophora* was principally associated with point source discharges of nutrients (e.g., sewage treatment plants, tributaries; Auer et al., 1982). The baseline map for Lake Huron created by this project also exhibited smaller, more isolated SAV patches. It is possible that these patches are associated with shoreline sources of nutrients or from the "nearshore shunt" driven by *Dreissena,* but availability of rock bottom would also continue to limit *Cladophora* extent.

4.1.3. Lake Erie

Lake Erie has the highest phosphorus levels of all of the Great Lakes and *Cladophora* there is considered to be governed by whole-lake nutrient levels, i.e., where hard substrate is present and light penetrates to the bottom, SAV thrives. However, a strong gradient in attenuation, relaxing from the western to eastern basin limits colonization by *Cladophora*. Much of the western basin, for example, could not be mapped using Landsat imagery because, with poor water clarity, the optically visible area of lake bottom is too narrow to be resolved by the satellite sensor. Field observations made in 2012, however, did not show dense *Cladophora* growth at depths greater than 2 m in the western basin, indicating a likely low total biomass of *Cladophora* in the western basin. The percentage of visible lake bottom in Lake Erie mapped as SAV was similar to the percentage for Lake Michigan, but the much smaller lake area and minimal bottom detection depth limit in much of the lake resulted in a lower mappable area and low total area of SAV. SAV in Lake Erie was most concentrated along the northern coast, particularly Long Point Bay and the Port Maitland area. Port Maitland was selected as a focal area for this project because it is an acknowledged *Cladophora* 'hotspot,' most likely due to nutrient loading from the Grand River. As with Lake Huron, the conditions supporting colonization and elevated biomass along the north shore cannot be confidently identified at this time, but may include regional and local phosphorus sources (e.g. the Grand River), phosphorus recycling by mussels and/or patchiness in hard substrate.

4.1.4. Lake Ontario

Lake Ontario has undergone dramatic reductions in phosphorus levels as a result of load management and has shifted from a system that is whole-lake forced with respect to *Cladophora* growth to one

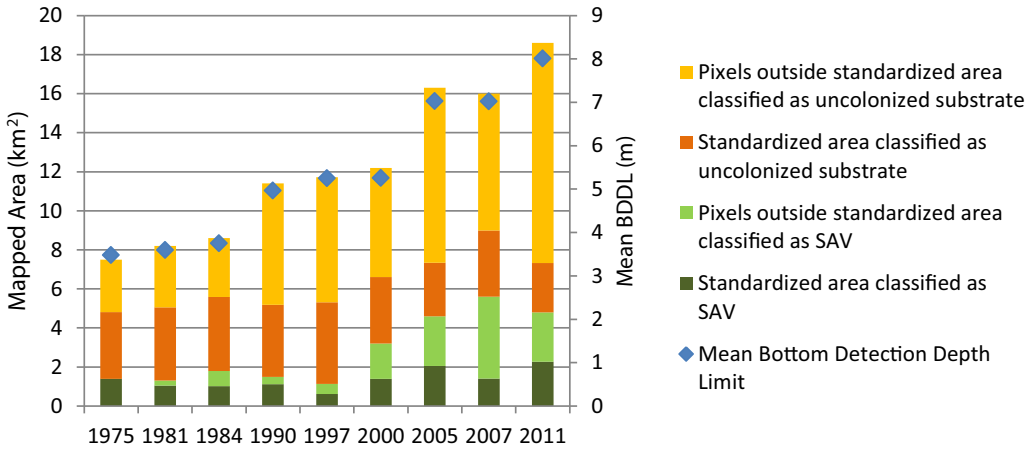

Fig. 9. The surface areas classified as SAV and as uncolonized substrate within and outside of the standardized lake bottom area, i.e., the pixels that were classifiable in all years of the time series, along the Ajax, ON shoreline (Lake Ontario) from the 1970s to the present. Darker colors represent standardized-area pixels and lighter colors nonstandardized-area pixels. Blue diamonds represent the mean water depth to which the bottom could be classified within the focus area.

where nuisance conditions are supported only where localized phosphorus enrichment occurs (Higgins et al., 2012). The fraction of the Lake Ontario nearshore zone mapped as SAV (40%), however, was still highest of all the lakes (Table 2), reflecting a combination of continuing phosphorus availability (higher than in Lakes Michigan and Huron) and the quality of the light environment (more suitable than in Lake Erie). Optical depth varied from 1-9 meters, increasing from the west side of the lake to the east. The densest SAV occurred near Toronto, ON, particularly in the Ajax area near the Pickering Nuclear Generating Station, and near the St. Lawrence River. Significant SAV growth was also observed along the southern shoreline west of Rochester, NY. Low SAV densities, i.e. a simple presence, are widely distributed around Lake Ontario but nuisance conditions are found only at sites with localized urban conditions (Higgins et al., 2012).

4.2. Time series analysis and the apparent role of dreissenid mussels in changing benthic vegetation dynamics

Based on the time series of Landsat imagery, trends in the percentage of SAV cover over time varied among lakes. When assessing only the area of lake bottom visible on all dates, the proportion of the visible lake bottom classified as SAV tended to increase over time at all areas of interest except the Bruce Peninsula (Lake Huron). Increases were more pronounced at the Milwaukee (Michigan) and Ajax (Ontario) sites and more gradual at Sleeping Bear (Michigan) and Port Maitland (Erie). Sleeping Bear, Ajax, and Port Maitland exhibited signs of a decrease in SAV extent in the late 1980s, coinciding with the basin-wide decline in ambient P driven by reduced nutrient loading (Nicholls, Hopkins, Standke, & Nakamoto, 2001), followed by more recent resurgences. This pattern across multiple sites lends support to our first hypothesis, that in at least some areas, reduced P loadings were effective at reducing the area of SAV cover until the introduction of exotic dreissenids. It is noteworthy that relative to most of the Great Lakes Basin, the percentages of urban and agricultural land uses within 2 km of the coast are particularly low along the western Bruce Peninsula (Hinchey & Cestaric, 2009). Thus, it is possible that local nutrient inputs along this part of the shoreline are low enough that SAV growth in this area has responded to the lake-wide decline in ambient phosphorus concentration.

At all sites except the Bruce Peninsula (Huron), the total mappable area and total area mapped as SAV began to increase immediately following the introduction of dreissenid mussels to the area, strongly supporting the study's second hypothesis. As an example, Fig. 4 places the change in total mapped area of SAV at Sleeping Bear Dunes in the context of the timing of the Great Lakes Water Quality Agreement and the appearance of zebra and quagga mussels. The increase in cover at Port Maitland began before 1990, which is slightly earlier than for the Lake Michigan sites; this could be linked to the earlier colonization of Lake Erie by dreissenid mussels compared to Lake Michigan. Dreissenid mussels were initially found in Lake St. Clair and Lake Erie in 1988 (Hebert, Muncaster, & Mackie, 1989) and became established in Lake Michigan in 1989 (Nalepa, Fanslow, & Lang, 2009). Both zebra and quagga mussels became established at similar dates in the Great Lakes (Mills et al., 1993; May & Marsden, 1992), with quagga mussels becoming more dominant in the Great Lakes by the mid-1990s (Mills et al., 1999). Variations among sites can presumably be attributed to a combination of differences in ambient phosphorus levels, local phosphorus sources, mussel density, water clarity, and hydrodynamics. Recent increases in the percent SAV cover in shallow areas may also represent a combination of more complete coverage of existing hard substrates and the colonization of new substrates in areas where sand or other soft substrates have been covered by mussel beds.

The bottom detection depth limit increased consistently across all sites over time, which corresponds to the basin-wide increases in water clarity. This increase in water clarity enabled the detection of increasingly deep substrates as the time series progressed. When the total area mapped as SAV, including the deep areas only visible in recent images, is considered, SAV cover is seen to increase at all sites except the Bruce Peninsula, where the total area of SAV has remained fairly stable. The percent cover of SAV along the Bruce Peninsula is still relatively high (18.5%), and the reflectance of much of the SAV patches is dark, indicating a dense standing crop. SAV is still reported to be a nuisance in the Bruce Peninsula area, but the problem is a combination of excessive growth of *Cladophora, Chara* and other periphyton. The variations among sites highlight the need for a more spatially extensive time series analysis. Lake-wide time series of SAV coverage would enable a better understanding of local benthic vegetation dynamics and place local patterns of change within a regional context.

Looking at Figs. 5 through 9, it is apparent that the recent resurgence in SAV growth has included both increases in cover in shallow areas and expansions into deeper water, supporting our final hypothesis. Along the shoreline, however, the current distribution of SAV is a combination of large dense patches at sites with a history of nuisance growth understood to be driven by localized P inputs (e.g., Milwaukee, Ajax) and new SAV patches at locations remote from known point sources (Sleeping Bear). This would suggest that although the link between local sources of P and SAV cover has weakened, point sources and high-P tributaries still play an important role in the basin-wide distribution of SAV.

5. Conclusions

A set of algorithms to map benthic vegetation (predominantly *Cladophora*) in the lower Great Lakes were developed and implemented, building from the work published in Shuchman, Sayers, et al., 2013. This new satellite approach to mapping the benthic environment of the entire visible nearshore Great Lakes was evaluated using field campaigns in all four of the lower Great Lakes at a total of 320 locations. We were then able to use this map to make initial estimates of SAV biomass in optically shallow water. The mean bottom detection depth limit varies among the lakes, being greatest in Lake Michigan (averaging approx. 12 m), intermediate in Lake Huron (9 m, lower in Saginaw Bay than in the rest of the lake) and lowest in Erie (4 m, excluding areas of the western basin that could not be mapped) and Ontario (approx. 6 m).

The Landsat time series dating back to 1973 was used as a virtual "time machine" to document changes in SAV extent over a four-decade period. The time series analysis found that bottom detection depth limit has slowly increased in recent decades, a phenomenon documented in earlier studies and attributed primarily to the filtering activities of non-native dreissenid mussels (e.g., Budd, Drummer, Nalepa, & Fahnenstiel, 2001). This increased water clarity has extended the colonizable area for *Cladophora* into progressively deeper water and has also allowed for satellite remote sensing of the lake bottom in increasingly deep water. In addition to new colonizing of deeper habitat, SAV patches appear to be increasing in size in most areas, most likely due to some combination of the nutrient recycling activities of mussels and the function of mussel shells as artificial reefs, which can provide new suitable substrate for growth.

Novel actions to reduce phosphorus loadings into the Great Lakes (e.g., enhanced waste water treatment and new guidelines for agricultural practices) are presently the only feasible means of addressing nearshore *Cladophora* problems such as avian botulism and beach fouling. Water quality managers will be challenged to quantify and defend the efficacy of proposed phosphorus control strategies given the associated financial burden. The results of this project, which mapped the extent of SAV and provided a timeline of the issue, will support managers and other Great Lakes stakeholders in making decisions related to SAV/*Cladophora* management in the Lakes by allowing them to prioritize management of problem areas and monitor the effectiveness of efforts in terms of the extent and biomass of vegetation.

The already 40-year-long time series of Landsat imagery will continue to be extended by Landsat 7, currently in operation, and the

Landsat Data Continuity Mission, successfully launched in February of 2013 and now known as Landsat 8. Continued monitoring of this problem in the Great Lakes will not only validate the efficacy of phosphorus control efforts but also help define complex relationships between terrestrial, pelagic and benthic energy and nutrient cycles. Furthermore, continued monitoring will aid in the understanding of the effects associated with other drivers such as invasive species, land use and climate change.

Acknowledgements

This project was funded by the USEPA-GLRI (Grant GL-00E00561-0). It expanded on a previous NASA-funded feasibility study (08-FEAS08-0025). The EPA Project Director was Jeffery May, and the NASA technical managers were Bradley Doorn and David Toll. During this project, the MTRI team collaborated with Great Lakes scientists from both governmental agencies and educational institutions. We would like to thank the following individuals for their advice and local expert domain knowledge: Dr. Martin Auer, Anika Kuczynski, Marcel Dijkstra, and Rasika Gawde (Michigan Tech University); Dr. Todd Howell (Environment Canada); Dr. Harvey Bootsma (University of Wisconsin, Milwaukee); Dr. Brenda M. Lafrancois (National Park Service); Ms. Alice Dove (Ontario Ministry of Environment).

Appendix A. Supplementary data

Supplementary data to this article can be found online at http://dx.doi.org/10.1016/j.rse.2014.04.032.

References

Andréfouët, S., Zubia, M., & Payri, C. (2004). Mapping and biomass estimation of the invasive brown algae *Turbinaria ornata* (Turner) J. Agardh and *Sargassum mangarevense* (Grunow) Setchell on heterogeneous Tahitian coral reefs using 4-meter resolution IKONOS satellite data. *Coral Reefs*, *23*, 26–38.

Auer, M. T., Tomlinson, L. M., Higgins, S. N., Malkin, S. Y., Howell, E. T., & Bootsma, H. A. (2010). Great Lakes *Cladophora* in the 21st century: Same alga – different ecosystem. *Journal of Great Lakes Research*, *36*, 248–255.

Auer, M. T., Canale, R. P., Grundler, H. C., & Matsuoka, Y. (1982). Ecological studies and mathematical modeling of *Cladophora* in Lake Huron: 1. Program description and field monitoring of growth dynamics. *Journal of Great Lakes Research*, *8*, 73–83.

Bootsma, H. A., Young, E. B., & Berges, J. A. (2004). Temporal and spatial patterns of *Cladophora* biomass and nutrient stoichiometry in Lake Michigan. In H. A. Bootsma, E. T. Jensen, E. B. Young, & J. A. Berges (Eds.), *Cladophora research and management in the Great Lakes. Special Report 2005-01*. (pp. 81–88). Milwaukee: Great Lakes Water Institute. University of Wisconsin.

Budd, J. W., Drummer, T. D., Nalepa, T. F., & Fahnenstiel, G. L. (2001). Remote sensing of biotic effects: Zebra mussels (*Dreissena polymorpha*) influence on water clarity in Saginaw Bay, Lake Huron. *Limnological Oceanography*, *46*, 213–223.

Bukata, R. P., Jerome, J. H., Kondratyev, A. S., & Pozdnyakov, D. V. (1995). *Optical properties and remote sensing of inland and coastal waters*. CRC press.

Byappanahalli, M. N., & Whitman, R. L. (2009). Clostridium botulinum type E occurs and grows in the alga *Cladophora glomerata*. *Canadian Journal of Fisheries and Aquatic Sciences*, *66*, 879–882.

Chambers, R. L., & Upchurch, S. B. (1979). Multivariate analysis of sedimentary environments using grain-size frequency distributions. *Journal of the International Association for Mathematical Geology*, *11*(1), 27–43.

Cherkauer, D. S., & Zvibleman, B. (1981). Hydraulic connection between Lake Michigan and a shallow ground-water aquifera. *Ground Water*, *19*(4), 376–381.

Congalton, R. G. (1988). A comparison of sampling schemes used in generating error matrices for assessing the accuracy of maps generated from remotely sensed data. *Photogrammetric Engineering & Remote Sensing*, *54*(5), 593–600.

Congalton, R. G., & Green, K. (2008). *Assessing the accuracy of remotely sensed data: principles and practices*. CRC Press.

Dekker, A. G., Brando, V. E., & Anstee, J. M. (2005). Retrospective seagrass change detection in a shallow coastal tidal Australian lake. *Remote Sensing of Environment*, *97*, 415–433.

Depew, D. C., Stevens, A. W., Smith, R. E., & Hecky, R. E. (2009). Detection and characterization of benthic filamentous algal stands(*Cladophora* sp.) on rocky substrata using a high-frequency echosounder. *Limnology and Oceanography: Methods*, *7*, 693–705.

DePinto, J. V., Lam, D., Auer, M., Burns, N., Chapra, S., Charlton, M., et al. (2006). Examination of the status of the goals of annex 3 of the Great Lakes water quality agreement. *Report of the Annex 3 model review sub-group to the GLWQA Review Working Group D – Nutrients*.

Depew, D. C., Houben, A. J., Guildford, S. J., & Hecky, R. E. (2011). Distribution of nuisance *Cladophora* in the lower Great Lakes: Patterns with land use, near shore water quality and dreissenid abundance. *Journal of Great Lakes Research*, *37*, 656–671.

Guenther, G. C., Cunningham, A. G., LaRocque, P. E., & Reid, D. J. (2000). Meeting the accuracy challenge in airborne lidar bathymetry. *EARSel-SIG-LIDAR Proceedings No. 1, Dresden, Germany*.

Fahnenstiel, G., Nalepa, T., & Pothoven, S. (2010). Lake Michigan lower food web: Long-term observations and *Dreissena* impact. *Journal of Great Lakes Research*, *36*, 1–4.

Graham, J. M., Auer, M. T., Canale, R. P., & Hoffmann, J. P. (1982). Ecological studies and mathematical modeling of *Cladophora* in Lake Huron: 4. Photosynthesis and respiration as functions of light and temperature. *Journal of Great Lakes Research*, *8*, 100–111.

Hebert, P. D. N., Muncaster, B. W., & Mackie, G. L. (1989). Ecological and genetic studies on *Dreissena polymorpha* (Pallas): a new mollusk in the Great Lakes. *Canadian Journal of Fisheries and Aquatic Sciences*, *46*, 1587–1591.

Hecky, R., Malkin, S., Ozersky, T., Depew, D., Houben, A., & Guildford, S. (2008). Dreissenid mussels in the Great Lakes and changes to nearshore nutrient ecology. *Paper presented at the 93rd ESA Annual Meeting; August 3–8 2008; Milwaukee, Wisconsin*.

Hecky, R. E., Smith, R. E. H., Barton, D. R., Guildford, S. J., Taylor, W. D., Charlton, M. N., et al. (2004). The near shore phosphorus shunt: a consequence of ecosystem engineering by dreissenids in the Laurentian Great Lakes. *Canadian Journal of Fisheries and Aquatic Sciences*, *61*, 1285–1293.

Herbst, R. P. (1969). Ecological factors and the distribution of *Cladophora glomerata* in the Great Lakes. *American Midland Naturalist*, *82*, 90–98.

Higgins, S. N., Malkin, S. Y., Howell, E. T., Guildford, S. J., Campbell, L., Hiriart-Baer, V., et al. (2008). An ecological review of *Cladophora glomerata* (Chlorophyta) in the Laurentian Great Lakes. *Journal of Phycology*, *44*, 839–854.

Higgins, S. N., Pennuto, C. M., Howell, E. T., Lewis, T. W., & Makarewicz, J. C. (2012). Urban influences on *Cladophora* blooms in Lake Ontario. *Journal of Great Lakes Research*, *38*, 116–123.

Higgins, S. N., Howell, E. T., Hecky, R. E., Guilford, S. J., & Smith, R. E. (2005). The wall of green: the status of *Cladophora glomerata* on the northern shores of Lake Erie's eastern basin, 1995–2002. *Journal of Great Lakes Research*, *31*, 547–563.

Hinchey, E. K., & Cestaric, R. (2009). Nearshore Areas of the Great Lakes 2009. *Background Paper for the State of the Lakes Ecosystem Conference 2008. EPA 905-R-09-013*.

Hochberg, E. J., & Atkinson, M. J. (2003). Capabilities of remote sensors to classify coral, algae, and sand as pure and mixed spectra. *Remote Sensing of Environment*, *85*, 174–189.

Knudby, A., Newman, C., Shaghude, Y., & Muhando, C. (2010). Simple and effective monitoring of historic changes in nearshore environments using the free archive of Landsat imagery. *International Journal of Applied Earth Observation and Geoinformation*, *12*, S116–S122.

Kutser, T. E., Vahtmäe, E., & Martin, G. (2006). Assessing suitability of multispectral satellites for mapping benthic macroalgal cover in turbid coastal waters by means of model simulations. *Estuarine, Coastal and Shelf Science*, *67*, 521–529.

Lekan, J. F., & Coney, T. A. (1982). The use of remote sensing to map the areal distribution of *Cladophora glomerata* at a site in Lake Huron. *Journal of Great Lakes Research*, *8*, 144–152.

Lyons, M. B., Phinn, S. R., & Roelfsema, C. M. (2012). Long term land cover and seagrass mapping using Landsat and object-based image analysis from 1972 to 2010 in the coastal environment of South East Queensland, Australia. *ISPRS Journal of Photogrammetry and Remote Sensing*, *71*, 34–46.

Lyons, M. B., Roelfsema, C. M., & Phinn, S. R. (2013). Towards understanding temporal and spatial dynamics of seagrass landscapes using time-series remote sensing. *Estuarine, Coastal and Shelf Science*, *120*, 42–53.

Lyzenga, D. R., Shuchman, R. A., & Arnone, R. A. (1979). Evaluation of an algorithm for mapping bottom features under a variable depth of water. *International Symposium on Remote Sensing of Environment, 13 th, Ann Arbor, Mich* (pp. 1767–1780).

Lyzenga, D. R. (1981). Remote sensing of bottom reflectance and water attenuation parameters in shallow water using aircraft and Landsat data. *International Journal of Remote Sensing*, *2*, 71–72.

Lyzenga, D. R., Malinas, N.P., & Tanis, F. J. (2006). Multispectral bathymetry using a simple physically based algorithm. *Geoscience and Remote Sensing, IEEE Transactions on*, *44*(8), 2251–2259.

Makarewicz, J. C., & Howell, E. T. (2012). The Lake Ontario Nearshore Study: Introduction and summary. *Journal of Great Lakes Research*, *38*, 2–9.

Malkin, S. Y., Bocaniov, S. A., Smith, R. E., Guildford, S. J., & Hecky, R. E. (2010). In situ measurements confirm the seasonal dominance of benthic algae over phytoplankton in nearshore primary production of a large lake. *Freshwater Biology*, *55*, 2468–2483.

Malkin, S. Y., Guildford, S. J., & Hecky, R. E. (2008). Modeling the growth response of *Cladophora* in a Laurentian Great Lake to the exotic invader *Dreissena* and to lake warming. *Limnological Oceanography*, *53*, 1111–1124.

May, B., & Marsden, J. E. (1992). Genetic identification and implications of another invasive species of dreissenid mussel in the Great Lakes. *Canadian Journal of Fisheries and Aquatic Sciences*, *49*, 1501–1506.

Mills, E. L., Dermott, R. M., Roseman, E. F., Dustin, D., Mellina, E., Conn, D. B., et al. (1993). Colonization, ecology, and population structure of the "Quagga" mussel (Bivalvia: Dreissenidae) in the Lower Great Lakes. *Canadian Journal of Fisheries and Aquatic Sciences*, *50*, 2305–2314.

Mills, E. L., Chrisman, J. R., Baldwin, B., Owens, R. W., O'Gorman, R., Howell, T., et al. (1999). Changes in the dreissenid community in the lower Great Lakes with emphasis on southern Lake Ontario. *Journal of Great Lakes Research*, *25*(1), 187–197.

Nalepa, T. F., Fanslow, D. L., & Lang, G. A. (2009). Transformation of the offshore benthic community in Lake Michigan: recent shift from the native amphipod Diporeia spp. to the invasive mussel *Dreissena rostriformis bugensis*. *Freshwater Biology*, *54*, 466–479.

Nalepa, T. F., & Schloesser, D. W. (Eds.). (2013). *Quagga and zebra mussels: Biology, impacts, and control*. CRC Press.

Neil, J. H., & Owen, G. E. (1964). *Distribution, environmental requirements and significance of Cladophora in the Great Lakes.* Ann Arbor, Michigan: Pub. #11, Great Lakes Research Div., The University of Michigan, 113–121.

Nevers, M. B., Byappanahalli, M. N., Edge, T. A., & Whitman, R. L. (2014). Beach science in the Great Lakes. *Journal of Great Lakes Research*, *40*, 1–14.

Nicholls, K. H., Hopkins, G. J., Standke, S. J., & Nakamoto, L. (2001). Trends in total phosphorus in Canadian near-shore waters of the Laurentian Great Lakes: 1976–1999. *Journal of Great Lakes Research*, *27*(4), 402–422.

North, R. L., Smith, R. E. H., Hecky, R. E., Depew, D. C., León, L. F., Charlton, M. N., et al. (2012). Distribution of seston and nutrient concentrations in the eastern basin of Lake Erie pre- and post-dreissenid mussel invasion. *Journal of Great Lakes Research*, *38*, 463–476.

Painter, S., & Kamaitis, G. (1987). Reduction in *Cladophora* biomass and tissue phosphorus in Lake Ontario, 1972–83. *Canadian Journal of Fisheries and Aquatic Sciences*, *44*, 2212–2215.

Piller, C., McArdle, S., & Patrick, P. H. (2008). Feasibility study on the Use of satellite imagery to identify submerged aquatic vegetation growth locations in the vicinity of Pickering nuclear generating station. *Report for Ontario Power Generation Inc. Produced by 4DM Inc. and SENES Consultants Limited.*

Rasmussen, J. L., Regier, H. A., Sparks, R. E., & Taylor, W. W. (2011). Dividing the waters: The case for hydrologic separation of the North American Great Lakes and Mississippi River Basins. *Journal of Great Lakes Research*, *37*, 588–592.

Rukavina, N. (1970). Lake Ontario nearshore sediments, Whitby to Wellington, Ontario. *Proceedings of the 13th Conference on Great Lakes Research* (pp. 266–272).

Schwab, D., & Sellers, D. (1996). Computerized bathymetry and shorelines of the Great Lakes (published 1980, revised 1996). *NOAA Data Report ERL GLERL-16, GLERL Contribution No. 212*. Ann Arbor, MI: Great Lakes Environmental Research Laboratory (http://www.glerl.noaa.gov/data/bathy/bathy.html, (6 pp)).

Sheath, R. G., Hambrook, J. A., & Nerone, C. A. (1988). The benthic macro-algae of Georgian Bay, the North Channel and their drainage basin. *Hydrobiologia*, *163*(1), 141–148.

Shuchman, R. A., Sayers, M. J., & Brooks, C. N. (2013a). Mapping and monitoring the extent of submerged aquatic vegetation in the Laurentian Great Lakes with multi-scale satellite remote sensing. *Journal of Great Lakes Research*, *39*(Supp. 1), 78–89.

Shuchman, R., Brooks, C., Sayers, M., Jessee, N., Grimm, A., Auer, M., et al. (2013). *Improved Cladophora monitoring through remote sensing: Final report for USEPA-GLRI grant GL-00E00561-0* (53 pp.).

Stewart, T. W., Miner, J. G., & Lowe, R. L. (1998). Quantifying mechanisms for zebra mussel effects on benthic macroinvertebrates: organic matter production and shell-generated habitat. *Journal of the North American Benthological Society*, *17*, 81–94.

Stewart, T. W., & Lowe, R. L. (2008). Benthic Algae of Lake Erie (1865–2006): A Review of Assemblage Composition, Ecology, and Causes and Consequences of Changing Abundance. *Ohio Journal of Science*, *108*(5), 82–94.

Taft, C. E., & Kishler, W. J. (1973). *Cladophora as related to pollution and eutrophication in western Lake Erie.* Columbus, Ohio: Water Resources Center, Ohio State University.

Thomas, R. L., Kemp, A. L., & Lewis, C. F. M. (1973). The surficial sediments of Lake Huron. *Canadian Journal of Earth Sciences*, *10*, 226–271.

Tomlinson, L. M., Auer, M. T., & Bootsma, H. A. (2010). The Great Lakes *Cladophora* Model: Development, testing, and application to Lake Michigan. *Journal of Great Lakes Research*, *36*, 287–297.

U.S. Environmental Protection Agency (EPA) (2008). Proceedings of the Great Lakes Basinwide Botulism Coordination Workshop: Appendix D. *EPA-950-R-08-005*. Chicago: US EPA Great Lakes National Program Office.

Vahtmäe, E., Kutser, T., Martin, G., & Kotta, J. (2006). Feasibility of hyperspectral remote sensing for mapping benthic macroalgal cover in turbid coastal waters – a Baltic Sea case study. *Remote Sensing of Environment*, *101*, 342–351.

Vodacek, A., & Raqueno, N. (2002). Algal bed patterns in the Rochester Embayment and along the western shoreline of Lake Ontario. *Lake Ontario Algae Cause and Solution Workshop, May 30, 2002, Greece, NY.*

Wezernak, C. T., & Lyzenga, D. R. (1976). Analysis of *Cladophora* distribution in Lake Ontario using remote sensing. *Remote Sensing of Environment*, *4*, 37–48.

Wolter, P. T., Johnston, C. A., & Niemi, G. J. (2005). Mapping submergent aquatic vegetation in the US Great Lakes using Quickbird satellite data. *International Journal of Remote Sensing*, *26*(23), 5255–5274.